complexation can also mediate solubility of flexible chain polymers just as was found for rigid-chain polymers.[1-3]

Unlike pure nylon 6, which is highly crystalline and opaque, the $GaCl_3$–nylon 6 complex is an optically transparent, amorphous material. Figure 2 shows the DSC

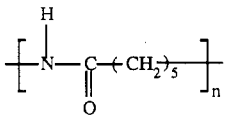

Nylon 6

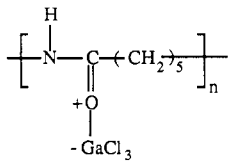

$GaCl_3$ · Nylon 6

thermograms for both the pure nylon and its $GaCl_3$ complex. The T_g of the complex is found to be 7 °C (midpoint) compared to a T_g value of 57 °C (midpoint) of the pristine nylon 6; this is a 50 °C reduction in T_g due to Lewis acid complexation of the polyamide. These values of the T_g of the pristine nylon 6 and its $GaCl_3$ complex were reproducible for several samples in three repeated heatings up to 120 °C and cooling. This significant shift in T_g after complexation sugests an increase in polymer free volume and segmental mobility of the polymer chains. In this respect, the $GaCl_3$–nylon 6 polymer complex is more like a polymer with a bulky "side chain" than a plasticized polymer, although chain branching[8,9] and plasticization[9] can each lead to a T_g reduction. The very low T_g of the complex compared to the pure nylon 6 also suggests the absence of hydrogen bonds in the $GaCl_3$–nylon 6 complex. Further substantiation of the lack of hydrogen bonding in the complex was obtained from FTIR data described below.

Table I shows the major bands and their assignment in the FTIR spectra of pure nylon 6 and its 1:1 $GaCl_3$ complex. The infrared bands of the pure nylon 6 in Table I are of the nylon 6 film regenerated from its $GaCl_3$ complex by precipitation in water. It is identical in all respects with the reported infrared spectrum for the pristine pure nylon 6.[10] This similarity of the infrared spectra of the nylon 6 recovered from its $GaCl_3$ complex and the pristine nylon 6 suggests the complete reversibility of the Lewis acid complexation. The complete recovery of the pure nylon 6 from its complex was further ascertained by the recovery of T_g, T_m, and insolubility in nitromethane. The pristine and regenerated nylon 6 samples were also insoluble, at 50–100 °C, in nitroalkanes, acetic acid, 3-chlorophenol, dimethyl sulfoxide, *N,N*-dimethylformamide, and chlorobenzene; hence intrinsic viscosity measurements could not be made to ascertain any possible change in molecular weight. These results show that the $GaCl_3$–nylon 6 solutions can be processed into the pure polymer films, coatings, or fibers. Furthermore, these results also suggest the feasibility of our envisioned processing of molecular composites of rigid-rod and flexible-chain polymers from ternary solutions of their complexes in organic solvents.[11]

A comparison of the FTIR spectra results for the pure nylon 6 and its $GaCl_3$ complex in Table I shows that the changes in the main bands are those anticipated for the severing of the N—H···O=C hydrogen bonds and complexation at the carbonyl oxygen site of the amide group. The N–H stretching band at 3293 cm^{-1} in the hydrogen-bonded nylon 6 is shifted to a higher frequency (by 70 cm^{-1}) in the complex. The amide I mode, which is known[12] to be dominated by the C=O absorption band, is shifted in the complex by 25 cm^{-1} to a lower frequency because of the greater electron-withdrawing effect of Lewis acid complexation at C=O than hydrogen bonding. Our FTIR results and their interpretation are confirmed by similar results and interpretation of the infrared spectra reported for BF_3 complexes of *N*-methylacetamide and related amide compounds.[13]

In conclusion, a stable 1:1 $GaCl_3$–nylon 6 complex has been prepared and found to be an optically transparent amorphous material in which the hydrogen bonds have been severed. The glass transition temperature of $GaCl_3$–nylon 6 was found to be reduced by 50 °C relative to the pure polymer. It was found that the pure nylon 6 was recoverable from its $GaCl_3$ complex by precipitation in water. These results demonstrate our concept of using Lewis acid complexation to modify polymer properties, mediate solubility and processing, and probe intermolecular interactions such as hydrogen bonding in polymers. Work in progress is investigating the Lewis acid–base chemistry of other aliphatic and aromatic polyamides, including solution- and solid-state properties of complexes and preparation of molecular composites.

Acknowledgment. We acknowledge support by grants from Amoco and General Electric Foundations.

(8) Nielsen, L. E. *Mechanical Properties of Polymers and Composites*; Marcel Dekker: New York, 1974; Vol. 1, pp 18–26.
(9) Duswalt, A. A. In *Plastics Polymer Science and Technology*; Baijal, M. D., Ed.; Wiley: New York, 1982; pp 201–237.
(10) Pouchert, C. J. *The Aldrich Library of FT-IR Spectra*, 1st ed.; Vol. 2, pp 1198–1200.
(11) Roberts, M. F., unpublished results. In preliminary studies, molecular composites of PBT and nylon 66 have actually been prepared from ternary solutions of their $GaCl_3$ complexes in nitromethane.
(12) Moore, W. H.; Krimm, S. *Biopolymers* **1976**, *15*, 2439.
(13) (a) Gerrard, W.; Lappert, M. F.; Wallis, J. W. *J. Chem. Soc.* **1960**, 2141. (b) Gerrard, W.; Lappert, M. F.; Pyszora, H.; Wallis, J. W. *J. Chem. Soc.* **1960**, 2144.

Preparation of Ultrathin, Size-Quantized Semiconductor Particulate Films at Oriented Mono- and Poly[(vinylbenzyl)phosphonate] Interfaces and Their Characterization on Solids

Youxin Yuan,[1] Israel Cabasso,*[,2] and Janos H. Fendler*[,1]

Department of Chemistry, Syracuse University Syracuse, New York 13244-1200 and State University of New York College of Environmental Science and Forestry Syracuse, New York 13210

Received February 2, 1990

We report here that vinylbenzyl phosphonate monomers and polymers, oriented at water–air interfaces, provide matrices for the size-controlled growth of semiconductor particles that can be transferred, essentially intact, onto solid substrates.

Preparations of $(C_{16}H_{35}O)_2P(=O)CH_2C_6H_4CH=CH_2$ (VBP), poly(styrenephosphonate diethyl ester) (PSP), and

(1) Syracuse University.
(2) Polymer Research Institute, State University of New York, College of Environmental Science and Forestry.

0897-4756/90/2802-0226$02.50/0

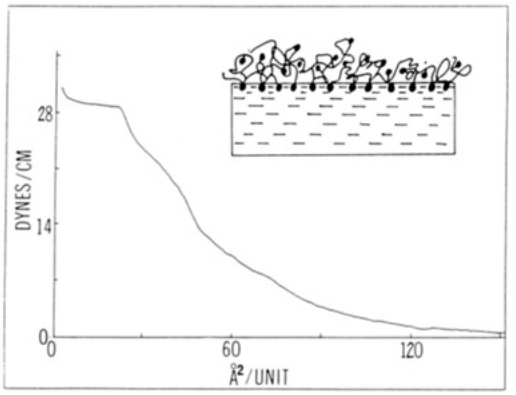

Figure 1. Surface pressure–surface area isotherm for PSP. The insert shows a possible alignment of the polymer on the water surface.

the 1:1 copolymer of PSP and poly(methyl methacrylate) (PSP:PMMA) have been described.[3,4] $Cd(NO_3)_2$, $Pb(NO_3)_2$, $ZnCl_2$, $InCl_3$ (Baker Analyzed Reagents), spectroscopic grade $CHCl_3$ (Aldrich), and H_2S (Matheson Gas Products) were used as received. Water was purified by using a Millipore Milli-Q filter system provided with a 0.2-μm Millistack filter at the outlet.

Appropriate amounts (20–50 μL) of 7.0×10^{-4} M VBP, PSP, or PSP:PMMA solutions in $CHCl_3$ were spread onto the clean surface of 1.0×10^{-3} M aqueous solutions of the desired metal salt.[5] Surface pressure–surface area curves (Figure 1) and assessment of the surface area occupied by the substrate established the formation of monomeric VBP, polymeric PSP, and copolymeric PSP:PMMA monolayers.[6] Slow infusion of H_2S resulted in the formation of semiconductor particles at the oriented monolayer–water interface. Nucleation at the surfactant headgroups was followed by two-dimensional particle growth to cover the entire monolayer. Subsequently, the particulate semiconductor film grew in thickness perpendicular to the plane of the monolayer. All of the incipient particles were supported by the monolayer, and there was no observable coloring (or semiconductor formation) in the

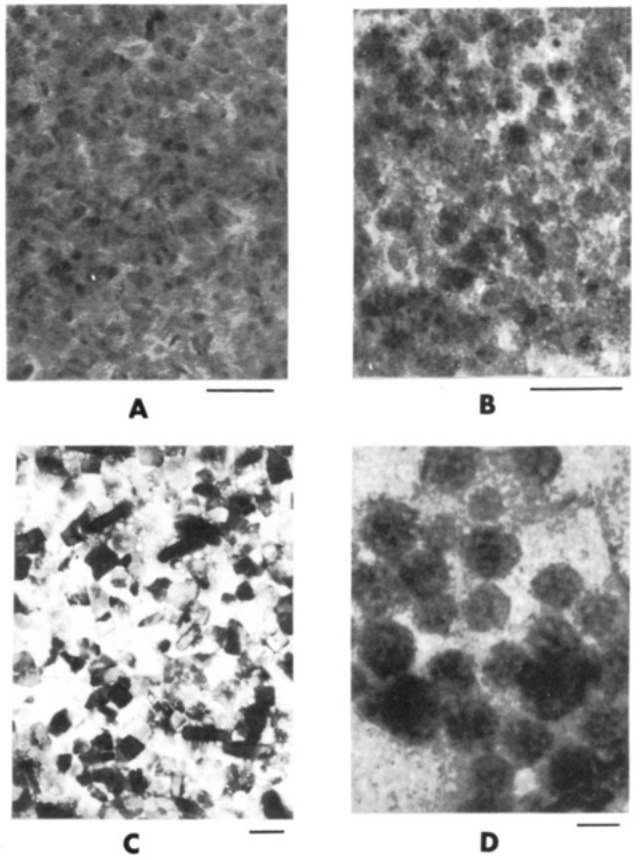

Figure 3. Transmission electron micrographs of CdS (A), ZnS (B), PbS (C), and In_2S_3 (D) formed on PSP polymer interfaces. The bar corresponds to 500 Å.

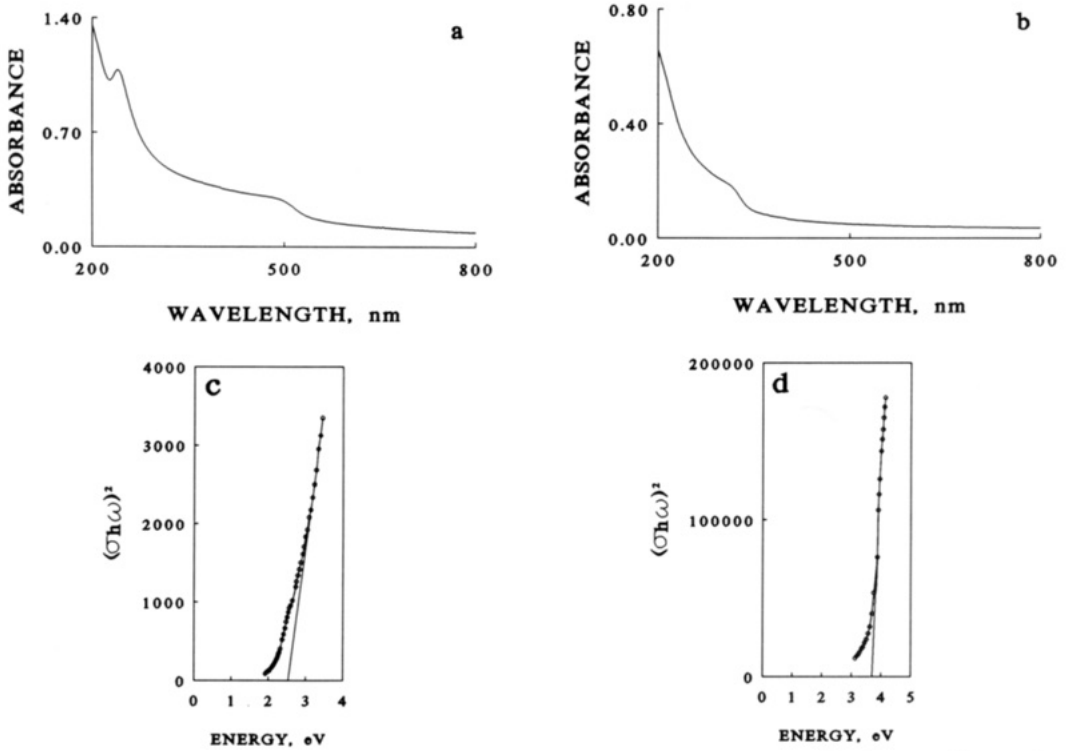

Figure 2. Absorption spectra of CdS (a) and ZnS (b), in situ generated in PSP interfaces and subsequently transferred to a quartz substrate. Plots of $(\sigma h\omega)^2$ against $h\omega$ (according to eq 3) are also shown for CdS (c) and ZnS (d). Intercepts of these plots gave the direct bandgap, E_g, of the semiconductor particulate film at the given thickness.

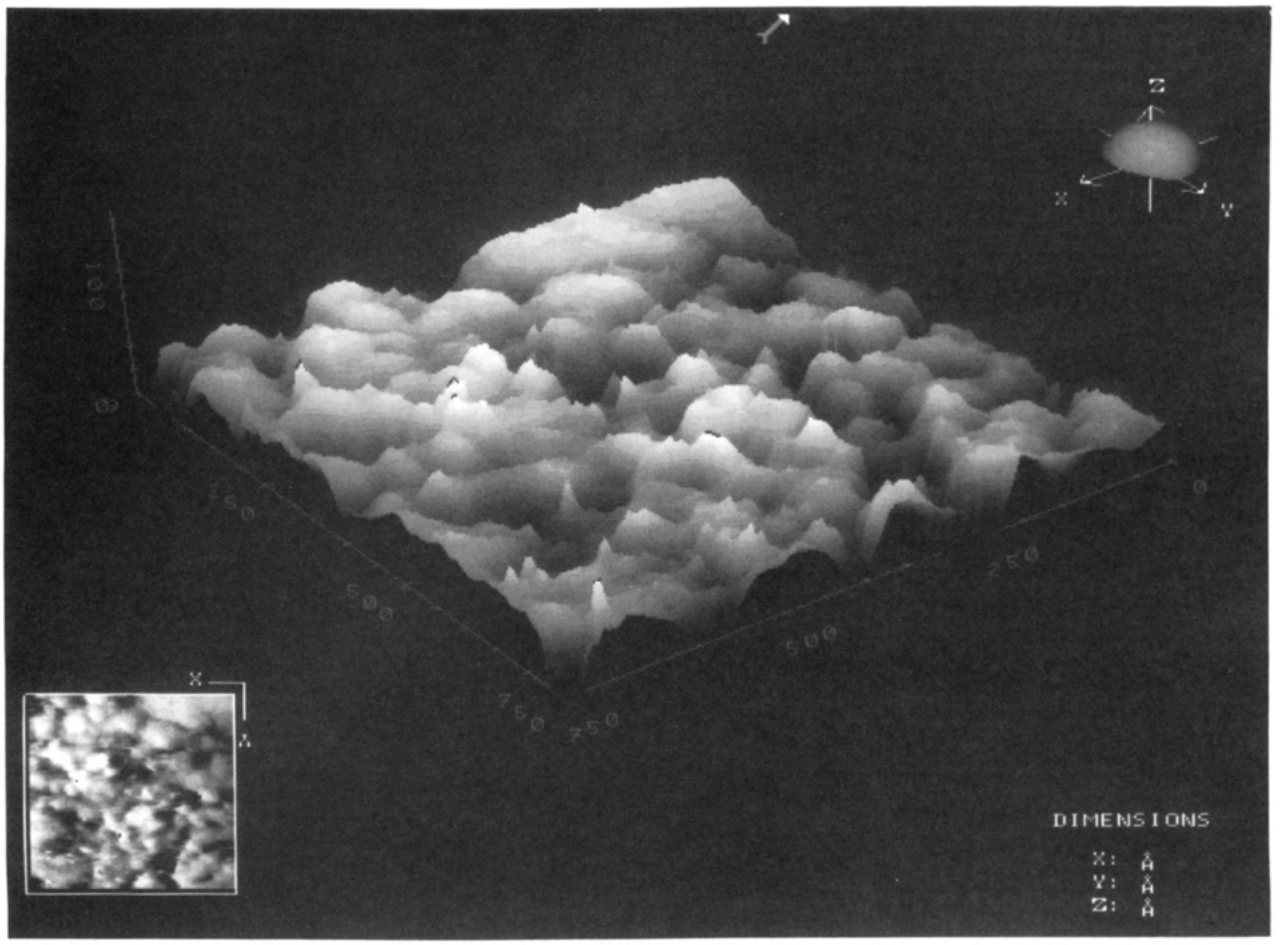

Figure 4. Constant current STM of 750 Å × 750 Å image of CdS particles. The particles were in situ formed at PSP polymer monolayer–water interfaces by exposure to H_2S (for ca. 20 min to form a 30 ± 5 Å thick particulate film) and subsequently transferred to HOPG. Figure 4 is a three-dimensional image; the insert shows a bird's-eye view of the same area in two dimensions (x and y axes are on the same scale as in the three-dimenisonal plot).

aqueous subphase. Strong electrostatic and particle–particle interactions are, presumably, responsible for maintaining the particulate semiconductor film at the monolayer interface. Formation and thicknesses of particles were monitored by reflectivity measurements on the monolayer surface.[7] The reflectivity and, hence, the optical thickness of the growing semiconductor particles increased steadily to a plateau value. The rate of growth and the optical thickness of the semiconductor particles formed depended markedly on the rate of H_2S infusion. In general, slower infusion of H_2S led to slower formation of thinner particles (Table I).

Dependence of the intensity of the reflected light on the incident angle (θ_0) at the monolayer–water interface prior (R_0) and subsequent to H_2S infusion (R_S) allowed the assessment of the effective refractive index of a given in situ grown semiconductor particulate film (n_s). The angle at which the θ_0 vs R_0 curve crossed the R_0 vs R_S was equated with the Brewster angle of the corresponding semiconductor particulate film (θ_B), which is, in turn, related to n_s by

$$n_s = \tan \theta_B \quad (1)$$

Values of n_s are considerably smaller than those determined for bulk crystalline semiconductors (Table I) and, hence, indicate the formation of a porous particulate

Table I. Semiconductor Particulate Film Formation at Mono- and Poly[(vinylbenzyl)phosphonate] Interfaces

matrix	semicond	time to reach plateau, min	d_S,[a] Å	n_S[b]	n_B[c]	F[d]
VBP	CdS	26[e]	680	2.14	2.53	0.67
PSP	CdS	120[f]	645	2.14	2.53	0.68
PSP	CdS	20[e]	840	2.14	2.53	0.68
PSP	ZnS	140[f]	780	1.77	2.38	0.36
PSP	PbS	200[f]	1100	2.56	3.92	0.60
PSP	In_2S_3	190[e]	500	1.86	3.90	0.22
PSP:PMMA	CdS	26[e]	680	2.14	2.53	0.69

[a] Optical thickness of the semiconductor particular film at the plateau of its formation. Calculated by using n_{PSP} = 1.48, n_{VBP} = 1.51, $n_{PSP:PMMA}$ = 1.44 determined separately.[7] [b] Effective refractive index of the semiconductor particular film. Determined by means of eq 1. [c] Refractive indices of bulk crystalline semiconductors taken from : *The Handbook of Chemistry and Physics*; CRC Press: Boca Raton, FL, 1988/89. [d] Fraction of particles on the semiconductor particulate film, calculated from eq 2, assuming the surrounding medium to be monomer and polymer molecules with n_m = 1.51, 1.48, and 1.44 for VBP, PSP, and PSP:PMMA, respectively. [e] H_2S injected into the subphase. [f] H_2S infused into the closed area surrounding the monolayer trough.

(3) Gardiner, E.; Cabasso, I. *Polymer* **1987**, *27*, 2052.

(4) Sun, J.; Cabasso, I. *J. Polym. Sci., Part A* **1989**, *27*, 3985. Sun, J. Ph.D. Thesis, State University of New York, College of Environmental Science and Forestry, 1989.

(5) Either a commercial Lauda Model P film balance or a circular, 50-mm-deep trough with a surface area of 69.4 cm^2 was used in these experiments.

(6) The viscosity average molecular mass, M_V, of PSP has been determined to be 23 000 by viscosity measurements. Taking 250 as the molecular weight of a polymer unit, we assess that ca. 90 of such units constitute the polymer. The surface area occupied per PSP headgroup was determined to be 25 $Å^2$/unit (see Figure 1), indicating an appreciable coiling of the polymer on the water surface.

(7) Reed, W.; Fendler, J. H. *J. Appl. Phys.* **1986**, *59*, 2914. Zhao, X. K.; Baral, S.; Rolandi, R.; Fendler, J. H. *J. Am. Chem. Soc.* **1988**, *110*, 1012.

semiconductor film.[8] The volume fraction of particles, F, was assessed from[9]

$$\frac{n_s^2 - n_m^2}{n_s^2 + 2n_m^2} = F\left(\frac{n_B^2 - n_m^2}{n_B^2 + 2n_m^2}\right) \quad (2)$$

where n_B and n_m are the refractive indexes of bulk crystalline semiconductors (Table I) and the surrounding medium. It is interesting to note that different particulate semiconductors organize themselves to different packing (see F values in Table I).

The semiconductor particulate films, formed at the mono- and poly[(vinylbenzyl)phosphonate] interfaces, were transferred to solid substrates by horizontal lifting. Well-cleaned quartz (chromic acid and dust-free water), celluloid-coated copper grids, and highly oriented pyrolytic graphite (HOPG, Union Carbide, freshly cleaved) were used for absorption spectrophotometry, transmission microscopy, and scanning tunneling microscopy, respectively.

Optical thicknesses of films on quartz prisms were also determined by reflectivity measurements. The optical thickness of a given particulate film on a glass prism was only 4–6% smaller than that determined on the monolayer surface prior to its transfer.

Absorption spectra of typical CdS and ZnS particulate films are shown in Figure 2. The simultaneous presence of fine structures (maxima and shoulders) and absorption edges situated at relatively long wavelengths is explicable by assuming the presence of a broad distribution of semiconductor particles, ranging from ultrasmall size-quantized[10] to relatively larger ones, in the particulate films. The broad size distribution, already observed in the thinnest film, remained essentially unaltered in the thicker films formed from the same semiconductor. Direct bandgaps, E_g values, were obtained from the intercepts of plots of the data according to eq 3, where σ is the ab-

$$(\sigma h\omega)^2 = h\omega C - E_g C \quad (3)$$

sorption coefficient ($A = \sigma d$ where A is the absorbance and d is the optical thickness of the semiconductor particulate film determined from reflectivity measurements) and $h\omega$ is the photon energy. Typical plots of the left-hand side of the equation against $h\omega$ are also shown in Figure 2. Values of E_g for CdS particulate films of d = 75, 130, 180, and 330 Å were assessed to be 2.59 (478 nm), 2.56 (485 nm), 2.49 (498 nm), and 2.44 eV (507 nm). Similarly, E_g values of ZnS particulate films of d = 110, 180, and 280 Å were calculated to be 3.71 (334 nm), 3.69 (336 nm), and 3.67 eV (338 nm). Values of 2.2 (558 nm) and 3.84 eV (323 nm) were similarly derived for the 270-Å-thick PbS and the 350-Å-thick In_2S_3 particulate films.

Transmission electron microscopy indicated the predominance of 75- and 80-Å-diameter particles of CdS and ZnS (Figure 3). In contrast, PbS appeared to form large cubic microcrystalline structures and the initially formed, very small In_2S_3 particles appeared to aggregate to larger structures (Figure 3).

Thin semiconductor particles, deposited on HOPG, were imaged in air by scanning tunneling microscopy (STM) using an Angstrom Technology (Mesa, AZ) Tak 3.0 instrument operated in the constant-current (1.0 nA) mode. STM images were scanned at five lines per second at ±500 mV tunneling voltage (tip vs substrate) and plotted on a CP 200 U Mitsubishi color video processor. STM images were taken on several separately prepared samples, and for each sample, data were taken at 10 different areas. The observed images showed particles with 20–30-Å widths and heights, which often formed loosely interconnecting structures (Figure 4).

In summary, functionalized monolayers have been shown to provide highly suitable matrices for the preparation of size-quantized particulate semiconductor films that could be transferred to a solid support. The methodology described here will allow the development of unique, nanosized electronic devices whose construction and examination are the subject of our current and intense scrutiny.

Acknowledgment. Support of this research by funds from the Center for Membrane Engineering and Science at Syracuse University is gratefully acknowledged.

(8) Zhao, X. K.; Baral, X.; Fendler, J. H. *J. Phys. Chem.* **1990**, *94*, 2043.

(9) Garnett, M. S. C. *Philos. Trans. R. Soc. London* **1904**, *203*, 385.

(10) Henglein, A. *Top. Curr. Chem.* **1988**, *143*, 113. Brus, L. A. *J. Phys. Chem.* **1986**, *90*, 2555. Andres, R. P.; Averback, R. S.; Brown, W. L.; Brus, L. E.; Goddard, W. A.; Kaldor, A.; Louie, S. G.; Moskovits, M.; Percy, P. S.; Riley, S. J.; Siegel, R. W.; Spaepen, F.; Wang, Y. *J. Mater. Res.* **1989**, *4*, 704.

Chromophore-Functionalized Polymeric Thin-Film Nonlinear Optical Materials. Effects of in Situ Cross-Linking on Second Harmonic Generation Temporal Characteristics

Joonwon Park and Tobin J. Marks*

Department of Chemistry and the Materials Research Center Northwestern University, Evanston, Illinois 60208

Jian Yang and George K. Wong*

Department of Physics and the Materials Research Center Northwestern University, Evanston, Illinois 60208

Received January 12, 1990

By increasing realizable chromophore number densities while impeding structural disorientation processes following electric field poling, chromophore-functionalized glassy polymers[1-3] represent an advance in macromolecular second harmonic generation (SHG) materials.[4] Nevertheless, structural relaxation/physical aging processes,[5,6] which erode poling-induced noncentrosymmetry and hence limit

(1) (a) Ye, C.; Marks, T. J.; Yang, Y.; Wong, G. K. *Macromolecules* **1987**, *20*, 2322–2324. (b) Ye, C.; Minami, N.; Marks, T. J.; Yang, J.; Wong, G. K. *Macromolecules* **1988**, *21*, 2901–2904. (c) Ye, C.; Minami, N.; Marks, T. J.; Yang, J.; Wong, G. K. In *Nonlinear Optical Effects in Organic Polymers*; Messier, J., Kajar, F., Prasad, P., Ulrich, D., Eds.; Kluwer Academic Publishers: Dordrecht, 1989; pp 173–183. (d) Hubbard, M. A.; Minami, N.; Ye, C.; Marks, T. J.; Yang, J.; Wong, G. K. *SPIE Proc.* **1989**, *971*, 136–143.

(2) Singer, K. D.; Kuzyk, M. G.; Holland, W. R.; Sohn, J. E.; Lalama, S. J.; Commizzoli, R. B.; Katz, H. E.; Schilling, M. L. *Appl. Phys. Lett.* **1988**, *53*, 1800–1802.

(3) (a) Eich, M.; Sen, A.; Looser, H.; Yoon, D. Y.; Bjorklund, G. C.; Twieg, R.; Swalen, J. D. *SPIE Proc.* **1989**, *971*, 128–135. (b) Eich, M.; Sen, A.; Looser, H.; Bjorklund, G. C.; Swalen, J. D.; Twieg, R.; Yoon, D. Y. *J. Appl. Phys.* **1989**, *66*, 2559–2567.

(4) (a) Messier, J., Kajar, F., Prasad, P., Ulrich, D., Eds. *Nonlinear Optical Effects in Organic Polymers*; Kluwer Academic Publishers: Dordrecht, 1989. (b) Khanarian, G., Ed. Nonlinear Optical Properties of Organic Materials. *SPIE Proc.* **1989**, *971*. (c) Heeger, A. J., Orenstein, J., Ulrich, D. R., Eds. Nonlinear Optical Properties of Polymers. *Mater. Res. Soc. Symp. Proc.* **1988**, *109*. (d) Chemla, D. S., Zyss, J., Eds. *Nonlinear Optical Properties of Organic Molecules and Crystals*; Academic Press: New York, 1987; Vols. 1 and 2. (e) Zyss, J. *J. Mol. Electron.* **1985**, *1*, 25–56. (f) Williams, D. J. *Angew. Chem., Int. Ed. Engl.* **1984**, *23*, 690–703.

0897-4756/90/2802-0229$02.50/0